LA-UR-95-1971

CONF-950720--10

Los Alamos National Laboratory is operated by the University of California for the United States Department of Energy under contract W-7405-ENG-36

TITLE: **ANALYSIS OF FUEL VAPORIZATION, FUEL/AIR MIXING, AND COMBUSTION IN LEAN PREMIXED/PREVAPORIZED COMBUSTORS**

AUTHOR(S): J. M. Deur, NYMA, Inc.
P. F. Penko, NASA Lewis Research Center
M(ichael) C. Cline, T-3

SUBMITTED TO: *31st AIAA/ASME/SAE/ASEE Joint Propulsion Conference, San Diego, California, July 10–12, 1995*

Los Alamos

Los Alamos National Laboratory
Los Alamos, New Mexico 87545

FORM NO. 836 R4
ST. NO. 2629 5/81

DISCLAIMER

Analysis of Fuel Vaporization, Fuel/Air Mixing, and Combustion in Lean Premixed/Prevaporized Combustors

J. M. Deur*
NYMA, Inc.
Brook Park, Ohio

P. F. Penko†
NASA Lewis Research Center
Cleveland, Ohio

M. C. Cline‡
Los Alamos National Laboratory
Los Alamos, New Mexico

Abstract

Requirements to reduce pollutant emissions from gas turbines used in aircraft propulsion and ground-based power generation have led to consideration of lean premixed/prevaporized (LPP) combustion concepts. This paper describes a series of the LPP combustor analyses performed with KIVA-II, a multi-dimensional CFD code for problems involving sprays, turbulence, and combustion. Modifications to KIVA-II's boundary condition and chemistry treatments have been made to meet the needs of the present study. The study examines the relationships between fuel vaporization, fuel/air mixing, and combustion in a generic LPP combustor. Parameters considered include: mixer tube diameter, mixer tube length, mixer tube configuration (straight versus converging/diverging tubes), air inlet velocity, air inlet swirl angle, secondary air injection (dilution holes), fuel injection velocity, fuel injection angle, number of fuel injection ports, fuel spray cone angle, and fuel droplet size. Cases have been run with and without combustion to examine the variations in fuel/air mixing and potential for flashback due to the above parameters. The degree of fuel/air mixing is judged by comparing average, minimum, and maximum fuel/air ratios at the exit of the mixer tube, while flame stability is monitored by following the location of the flame front as the solution progresses from ignition to steady state.

Background

Nitrogen oxides (NO_x) are serious contributors to air pollution, and considerable engineering effort is being expended to reduce their emission from gas turbine combustors used in aircraft propulsion and ground-based power generation. This has led to a growing interest in lean combustion, as NO_x formation is reduced substanially at lower equivalence ratios. An LPP system (Fig. 1A) further limits emissions by separating the fuel vaporization and fuel/air mixing processes from the final combustion process to eliminate non-uniformities in the fuel/air mixture, thus eliminating hot spots where high levels of NO_x are formed. Unfortunately, lean combustion devices have some drawbacks, particularly with regards to flame stability.[1]

Numerical analyses of a generic LPP combustor are being conducted to examine the role of geometry and various inflow parameters on fuel/air uniformity and flame stability. The calculations in this study utilize a simple cylindrical configuration (Fig. 1B) consisting of a straight tube with a "hypodermic needle" fuel injector. In this tube, the fuel (Jet-A) is introduced, vaporized, and combined with the inlet air. The fuel/air mixture is then dumped into a larger cylinder where the combustion takes place.

Numerical Method

The calculations are performed with KIVA-II, a CFD program developed originally to study the in-cylinder combustion dynamics of internal combustion engines. However, because the code can treat problems combining sprays, turbulence, and com-

---

* Supervisor, Combustion and Icing Section. Senior Member AIAA.

† Aerospace Engineer. Member AIAA.

‡ Staff Member, Group T-3. Member AIAA.

bustion, it can be employed in the analysis of gas turbine combustors as well.[2,3,4]

KIVA-II describes fuel sprays with a stochastic model applied to discrete computational particles representing collections of droplets with identical physical properties (size, temperature, velocity, etc.). These particles interact with the surrounding fluid, exchanging mass, momentum, and energy as the droplets travel downstream and evaporate. The spray model also incorporates sub-models for droplet collisions, turbulent dispersion, and aerodynamic breakup. In practice, it has been found that the collision and breakup sub-models are too efficient, rapidly skewing droplet distributions to the smaller sizes in an unrealistic fashion. As a result, these two models are not used in this series of calculations.

To characterize turbulence within the flowfield, KIVA-II employs a standard k-ε model with wall functions.

KIVA-II can accept an arbitrary reaction set and incorporates a quasi-equilibrium option to split fast and slow reactions between equilibrium and finite-rate kinetics, respectively. However, as originally released, KIVA-II is limited to laminar kinetics. For this study, the mixing-controlled combustion model of Magnussen and Hjertager has been added to portray the combustion/turbulence interaction. This model is used in conjunction with the simplified reaction scheme developed by Ying and Nguyen to describe the combustion chemistry.[5,6]

Owing to its origins, KIVA-II's ability to treat some of the geometries to be examined in this study is also limited. To rectify this, the program's boundary condition treatment has been revised to allow incorporation of dilution jets, non-vertical walls, and inflow/outflow boundary planes with mixtures of open and closed grid cells.

Grids and Boundary Conditions

A variety of grids are used in this study, almost all generated by using KIVA-II's internal grid generation routines. The grid for the baseline case (Figs. 2A and 2B) is a uniform cylindrical mesh. Due to symmetry, only a 180° half-cylinder is needed, leading to a 27x19x205 mesh in cases when the dump section is included and a 11x19x151 mesh when only the mixer tube is used. Cell spacing is chosen, in part, such that the dilution holes near the mixer tube exit can be approximated by 2x2 clusters of cells. The rectangle formed by these cells has 93% of the area and 93% of the width of the original circular dilution hole.

To test some geometry variables and inlet conditions, modifications have to be made to the baseline grid. For cases involving converging/diverging mixer tubes, radial cell spacing in successive K-planes (I, J, and K grid indices correspond to r, θ, and z directions in cylindrical coordinates) are linearly varied to produce the desired venturi geometry. Cases involving inlet air swirl require full 360° grids, since the symmetry plane is lost.

To study the flow blockage associated with the fuel injection tube, an externally generated grid is employed that explicitly models the tube (Fig. 2C). To reduce grid effects and return to the mesh needed to represent the downstream dilution holes, the cell spacing in successive K-planes downstream of the injection tube is slowly returned to the uniform baseline distribution.

For all cases examined, the air inlet temperature and pressure are 1100° F and 11.5 atm, respectively. For the baseline case, the total air mass flow rate is 0.161 lbm/sec, with 88.5% of the flow entering through the base of the mixer tube and the remainder split equally amongst the dilution holes ringing the tube near its downstream exit. The overall fuel/air ratio is 0.033. The fuel is injected at a velocity of 52.7 fps, with a droplet SMD of 20 μm and a spray cone angle of 20°.

Analysis

To quantify the degree of mixing, three exit plane fuel/air ratios will be reported: minimum, maximum, and average. The first two are simply the minimum and maximum values found amongst the grid cells located at the exit plane of the mixer tube, while the average value is a spatial or cell average across the exit plane. The spatial average is more revealing than the mass average would be, since the latter will just equal the overall fuel/air ratio, a constant in these calculations. On the other hand, the spatial average will vary with the distribution of fuel vapor across the exit plane owing to the variation in cell density. If the fuel is concentrated near the center of the tube (Region A in Fig. 2D), the average will be relatively high, since there is a greater cell density near the tube's center. However, if there is more fuel near the wall (Region B), the average will be relatively low, due to the lower cell density near the wall.

In all cases, the three reported fuel/air ratios are averages over a number of cycles, typically 1,000, to account for the random changes in the fuel/air ratio at the exit plane due to the stochastic spray model. Since the distribution of droplets intro-

duced by the spray model varies as a random variable, the fuel/air distribution also varies over time. Thus, to obtain representative values for the fuel/air ratio, time averaging is required.

Results

To date, 39 analyses have been completed (Table 1), examining the effects of a variety of parameters on fuel/air mixing and, to a lesser extent, on combustion in the generic LPP combustor.

Fuel Injection Tube

In most of the calculations presented here, the flow blockage due to the fuel injection tube is not represented. To examine what effect this blockage might have on fuel/air mixing, an analysis of the baseline configuration with the fuel injection tube included has been performed to allow a side-by-side comparison to be made (Fig. 3). While the axial velocity field immediately behind the injection tube is strongly disturbed, there is little effect on the fuel spray pattern and, consequently, relatively little effect on the fuel/air distribution. While there is some enhanced mixing in that half of the mixer tube downstream of the injection tube, there is insufficient fuel in that region to strongly effect the overall fuel/air distribution.

Fuel Droplets and Sprays

In the next series of analyses, the fuel injection angle is varied from the baseline's 15° to 90°, i.e., from roughly perpendicular to the inlet air flow to parallel to that flow (Fig. 4). Initially, there is relatively little change, until the angle increases to where the spray impingement on the mixer tube wall is removed. As the angle increases from that point, there is substantial improvement in overall mixture uniformity. The star-shaped pattern in the exit plane fuel/air ratio at 90° (Fig. 4B) results from the dilution hole inflow.

A similar improvement in uniformity is obtained by reducing the fuel injection velocity (Fig.5). Curiously, increasing the injection velocity also reduces the maximum exit plane fuel/air ratio. However, the minimum fuel/air ratio in this case is reduced far more, indicating that overall non-uniformity at the higher injection velocity is still increased. The decrease in the maximum fuel/air ratio may be a result of the higher injection velocity displacing the spray cone outward such that the mixer tube wall cuts across a broader section of the cone.

Perhaps surprisingly, droplet size has little effect on mixing, at least over the ranges of sizes considered here (Fig. 6). However, the fuel droplet population results may point to increased uniformity at smaller droplet sizes, since it appears that vaporization is becoming so fast that impingement with the wall may be avoided altogether. Of course, such smaller sizes may not be physically realizable.

These last two series of calculations point to an unexpected advantage of numerical analysis. Given the structure of KIVA-II, it is possible to vary independently parameters that, in reality, are closely coupled, e.g., fuel injection velocity and fuel droplet SMD. This permits separate evaluations of these parameters to be made that cannot be performed experimentally

The final spray parameter to be considered is the spray cone angle (Fig. 7). As might be expected, increasing the cone angle improves the degree of fuel/air uniformity.

Air Inflow

Turning to modifications of the air inflow, the first set of analyses examines the addition of a venturi effect (Fig. 8). In this series, the throat of the venturi is at the same axial station as the fuel injection. The level of constriction is defined as the minimum to maximum tube radius ratio. Three ratios, from 0.5 to 0.75, have been considered to date. As anticipated, increasing the throat constriction substantially increases the fuel/air uniformity at the exit plane of the mixer tube. However, aerodynamic choking at the throat limits the degree of constriction permissible. In the present study, the 0.5 radius ratio chokes the flow at the venturi throat.

Inlet air swirl is another means of improving fuel/air mixing. Swirl angles from 30° to 60° have been considered in this study (Fig. 9), with the best mixing found at highest angle.

In practice, swirl and venturi effects are often combined. Unfortunately, the baseline conditions in the present study have made this combination somewhat difficult to evaluate, since even modest amounts of swirl combined with the flow acceleration from the flow constriction of the venturi leads to choked flow. In fact, only the most moderate combinations of the parameter values already considered in the present study avoid choking (Fig.10). However, this case does demonstrate that the combination of swirl with flow constriction can improve mixing more than either alone.

Dilution Holes

It has been found that relocating the dilution holes from the mixer tube exit to the axial station where the fuel injection occurs has almost the same effect as an equivalent venturi tube configuration (Fig. 11). By examining the disturbance to the mean flow created by the dilution holes, it is found that they represent a 20% reduction in flow area, or the equivalent of a 0.9 radius ratio venturi tube. Mapping their effect on the exit plane fuel/air ratios at this equivalent radius ratio on the venturi tube graph shows that their effect is almost identical to what could be expected for the corresponding venturi tube configuration.

Removing the dilution holes altogether also affects the degree of mixing uniformity (Fig. 12). First, to maintain the overall fuel/air ratio, the inflow velocity at the base of the mixer tube must be increased, leading to a slight reduction in the degree of penetration of the fuel spray and a small increase in the downstream distance through which the fuel droplets are convected before vaporizing. These same effects would result if the fuel injection velocity were to be reduced. Based on the effect that reducing fuel injection velocity has on mixing (Fig. 5), this increase in the air velocity could be expected to improve the fuel/air distribution at the mixer tube exit, but the exit plane values show that mixing is actually slightly poorer without the dilution holes. The direct mixing effect that the dilution holes provide outweighs the slight losses due to the consequently lower air inlet velocity at the mixer tube entrance.

Multiple Fuel Nozzles

Increasing the number of fuel injection nozzles substantially improves the fuel/air distribution at the exit of the mixer tube (Fig. 13). An additional case shows that staggering the nozzles, in this instance by an inch, does not appreciably affect the degree of uniformity at the exit plane. The slight increase in non-uniformity is likely due to the downstream displacement of the second nozzle.

Mixer Tube Length Effects

Reducing the mixer tube length moves the fuel injection point closer to the tube exit, consequently leaving less distance for fuel/air mixing to be performed. Calculations in this series show the decreasing uniformity as the mixer tube is shortened (Fig. 14). The results for the 50% baseline case are even poorer than the exit plane plot indicates, since a small number of droplets are leaving the tube without vaporizing. Thus, there is a small amount of fuel unaccounted for in the fuel/air ratio calculations, since they only consider vaporized fuel.

Mixer Tube Diameter

In considering changes in mixer tube diameter, the effect on the mass flow rate of air entering the tube has to be taken into account. Two approaches are considered here. In the first, the flow rate is held constant by reducing in the velocity of the air entering the tube (Fig. 15). In the second, the inlet velocity is held constant, leading to an increase in the air mass flow which is balanced by increasing the fuel mass flow rate to hold the overall fuel/air ratio constant (Fig. 16). In both cases, increasing mixer tube diameter increases non-uniformity.

As decreasing flow velocities promote flashback, the calculations involving mixer tubes of increasing diameter, but fixed mass flow, has been extended to include combustion (Fig. 17). Excepting the baseline case, all show some evidence of flashback, but the flashback is limited to a small region downstream of the two dilution holes on either side of the fuel injection plane. It appears that the adverse pressure gradient immediately downstream of these holes leads to a reverse flow that draws the flame front back into the mixer tube. The poor fuel/air distribution within the tube probably explains why no flashback is observed around the other dilution holes; there is simply insufficient fuel to support combustion around them.

There is also a periodic character to the observed flashback phenomenon (Fig. 18). Although the exact mechanism is not yet clear, a potential explanation can be proposed: When the flame enters the tube, it heats a pocket of gas within the tube, causing the flow in the tube to accelerate. The faster flow then drives the flame back out of the tube. The flow within the tube then decelerates to the point where the flame can re-enter, beginning the cycle again. The dilution holes, in addition to providing the path for the flame to enter the tube, also stop it from proceeding further into the tube.

Conclusions

A series of calculations have been performed which quantify the effects of a number of parameters on the degree of fuel/air mixing uniformity achieved in a generic LPP combustor. The biggest gains in uniformity are achieved through a combina-

tion of air inlet swirl and venturi tube geometry. Multiple fuel injection points also promote good mixing. A limited series of calculations have examined flashback in mixer tubes with larger diameters, but fixed mass flows. In these cases, flashback appears to be strongly affected by the presence of the dilution holes near the mixer tube exit.

Additional calculations are underway to further examine flashback in the mixer tube, particularly with regards to the role of the dilution holes. Other calculations will study the effects of additional parameters on fuel/air mixing.

References

[1]Deur, J. M., Kundu, K. P., Darling, D. D., Cline, M. C., Micklow, G. J., Harper, M. R., and Simons, T. A., "Analysis of Lean Premixed/Prevaporized Combustion with KIVA-II, AIAA Paper 94-3895, August 1994.

[2]Amsden, A. A., O'Rourke, P. J., Butler, T. D., "KIVA-II: A Computer Program for Chemically Reacting Sprays with Sprays," LA-11560-MS, Los Alamos National Laboratory, Los Alamos, New Mexico, May 1989.

[3]Deur, J. M., Kundu, K. P., Nguyen, H. L., "Applied Analytical Combustion/Emissions Research at the NASA Lewis Research Center: A Progress Report," AIAA Paper 92-3338, July 1992.

[4]Cline, M. C., Deur, J. M., Micklow, G. J., Harper, M. R., and Kundu, K. P., "Computation of the Flowfield in an Annular Gas Turbine Combustor," AIAA Paper 93-2074, June 1993.

[5]Magnussen, B. F., and Hjertager, B. H., "On Mathematical Modeling of Turbulent Combustion with Special Emphasis on Soot Formation and Combustion," *Proceedings of the 16th Symposium on Combustion*, The Combustion Institute, Pittsburgh, Pennsylvania, 1977, pp. 719-729.

[6]Ying, S. L., and Nguyen, H. L., "Numerical Simulation of Jet-A Combustion Approximated by Improved Propane Chemical Kinetics," AIAA Paper 91-1859, June 1991.

Table I. Summary of KIVA-II Analyses of Generic LPP Combustor.

CASE	DESCRIPTION	f/a_{min}	$f/a_{avg} \times 10^{-2}$	$f/a_{max} \times 10^{-1}$	REMARKS
1	BASELINE	2.1597×10^{-8}	2.6903	2.7039	
2	BASELINE WITH INJECTION TUBE	3.7385×10^{-5}	2.9617	2.4949	
3	FUEL INJECTION ANGLE = 45°	2.6170×10^{-8}	2.7389	2.6609	
4	FUEL INJECTION ANGLE = 75°	2.6637×10^{-7}	4.4655	2.1535	
5	FUEL INJECTION ANGLE = 90°	2.9765×10^{-4}	5.2166	1.2620	
6	FUEL INJECTION VELOCITY = 13.2 fps (25% BASELINE)	2.1957×10^{-7}	4.2111	1.8509	
7	FUEL INJECTION VELOCITY = 26.4 fps (50% BASELINE)	6.7068×10^{-8}	3.3612	2.0005	
8	FUEL INJECTION VELOCITY = 79.1 fps (150% BASELINE)	4.8816×10^{-9}	2.4879	2.4279	
9	FUEL DROPLET SMD = 10 μm (50% BASELINE)	2.6918×10^{-8}	2.7739	2.3131	
10	FUEL DROPLET SMD = 30 μm (150% BASELINE)	6.6309×10^{-9}	2.6183	2.7366	
11	FUEL DROPLET SMD = 40 μm (200% BASELINE)	6.4358×10^{-9}	2.3593	2.4803	
12	FUEL SPRAY CONE ANGLE = 40° (200% BASELINE)	2.0279×10^{-8}	2.7085	2.3576	
13	FUEL SPRAY CONE ANGLE = 60° (300% BASELINE)	2.7403×10^{-8}	2.9173	2.0339	
14	VENTURI WITH $r_{min}/r_{max} = 0.50$	—	—	—	CHOKED FLOW
15	VENTURI WITH $r_{min}/r_{max} = 0.67$	2.0949×10^{-4}	3.2765	1.4479	
16	VENTURI WITH $r_{min}/r_{max} = 0.75$	1.9695×10^{-6}	2.7397	1.7951	
17	INLET AIR SWIRL ANGLE = 30°	1.2793×10^{-5}	3.2689	1.2340	
18	INLET AIR SWIRL ANGLE = 45°	1.9663×10^{-4}	3.5690	0.9629	
19	INLET AIR SWIRL ANGLE = 60°	2.4735×10^{-3}	3.6908	0.7594	
20	VENTURI WITH $r_{min}/r_{max} = 0.67$ AND INLET AIR SWIRL ANGLE = 30°	—	—	—	CHOKED FLOW
21	VENTURI WITH $r_{min}/r_{max} = 0.67$ AND INLET AIR SWIRL ANGLE = 45°	—	—	—	CHOKED FLOW
22	VENTURI WITH $r_{min}/r_{max} = 0.67$ AND INLET AIR SWIRL ANGLE = 60°	—	—	—	CHOKED FLOW

Table I. Summary of KIVA-II Analyses of Generic LPP Combustor (Continued).

CASE	DESCRIPTION	f/a_{min}	$f/a_{avg} \times 10^{-2}$	$f/a_{max} \times 10^{-1}$	REMARKS
23	VENTURI WITH r_{min}/r_{max} = 0.75 AND INLET AIR SWIRL ANGLE = 30°	2.1444×10^{-4}	3.2323	0.8606	
24	VENTURI WITH r_{min}/r_{max} = 0.75 AND INLET AIR SWIRL ANGLE = 45°	—	—	—	CHOKED FLOW
25	VENTURI WITH r_{min}/r_{max} = 0.75 AND INLET AIR SWIRL ANGLE = 60°	—	—	—	CHOKED FLOW
26	COPLANAR FUEL INJECTION NOZZLE AND DILUTION HOLES	1.4749×10^{-5}	2.9546	2.1826	
27	NO DILUTION HOLES	6.5459×10^{-9}	2.5602	2.8792	
28	2 FUEL INJECTION NOZZLES (WITH 1 INCH AXIAL STAGGER)	1.6801×10^{-5}	3.1653	1.1776	
29	2 FUEL INJECTION NOZZLES (COPLANAR)	4.1168×10^{-5}	3.2658	1.0297	
30	4 FUEL INJECTION NOZZLES (COPLANAR)	1.9022×10^{-3}	4.3945	0.8327	
31	MIXER TUBE LENGTH = 2.75 in (50% BASELINE)	6.3107×10^{-11}	2.5576	4.3819	
32	MIXER TUBE LENGTH = 4.14 in (75% BASELINE)	2.0103×10^{-9}	2.5349	3.3000	
33	BASELINE WITH DUMP (NO COMBUSTION)	2.5784×10^{-8}	2.7275	2.8820	
34	BASELINE WITH DUMP (WITH COMBUSTION)	1.6875×10^{-8}	2.7103	3.0010	NO FLASHBACK
35	MIXER TUBE DIAMETER = 0.75 in WITH m_{air} = c (150% BASELINE)	3.6792×10^{-8}	2.5327	3.6781	FLASHBACK
36	MIXER TUBE DIAMETER = 1.00 in WITH m_{air} = c (200% BASELINE)	1.4869×10^{-9}	2.4971	4.0303	FLASHBACK
37	MIXER TUBE DIAMETER = 1.25 in WITH m_{air} = c (250% BASELINE)	2.2122×10^{-9}	2.3595	3.7886	FLASHBACK
38	MIXER TUBE DIAMETER = 0.75 in WITH v_{air} = c (150% BASELINE)	6.6383×10^{-12}	2.6131	3.7119	
39	MIXER TUBE DIAMETER = 1.00 in WITH v_{air} = c (200% BASELINE)	9.4127×10^{-15}	2.5139	4.5456	

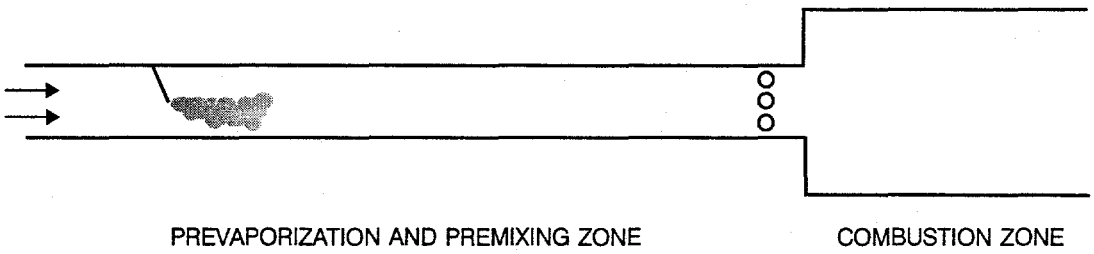

A. Schematic Diagram.

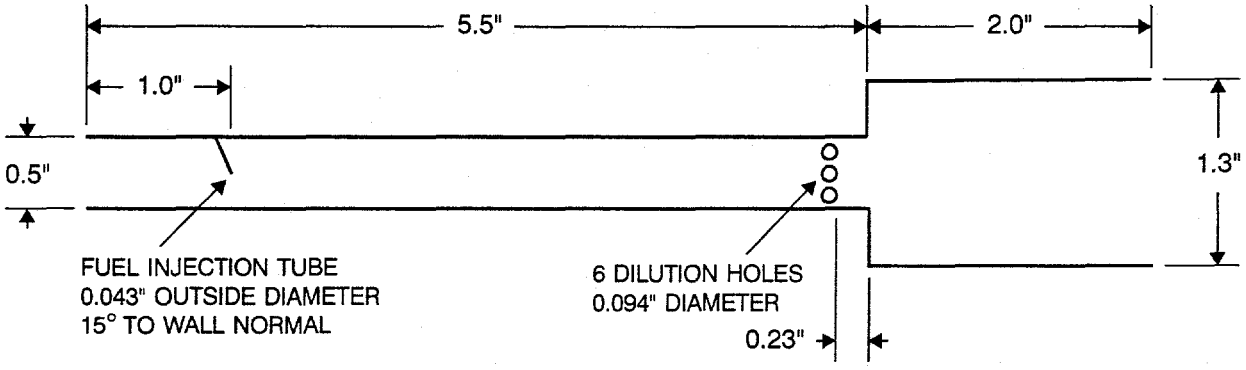

B. Dimensions for Baseline Case.

Figure 1. Generic LPP Combustor.

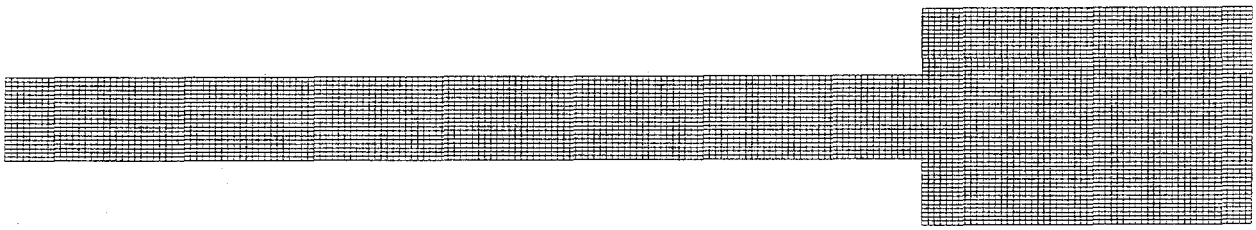

A. J-Plane.

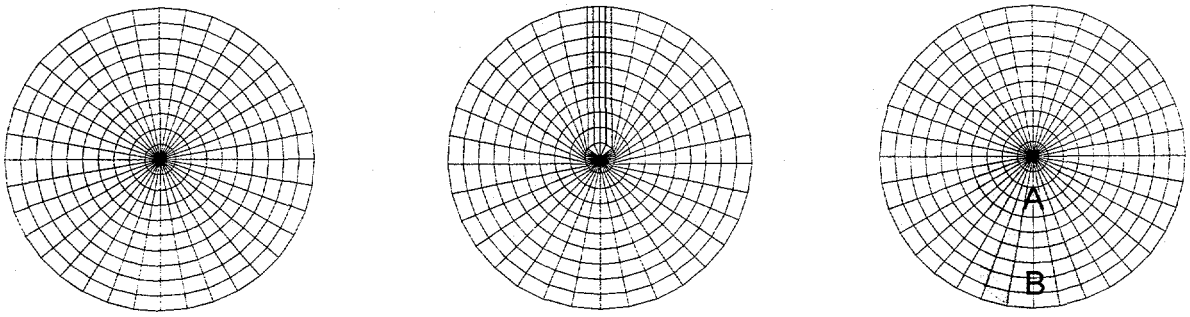

B. K-Plane without Fuel Tube. C. K-Plane with Fuel Tube. D. Fuel/Air Ratio Patterns.

Figure 2. Grid Characteristics for KIVA-II Analyses of Generic LPP Combustor.

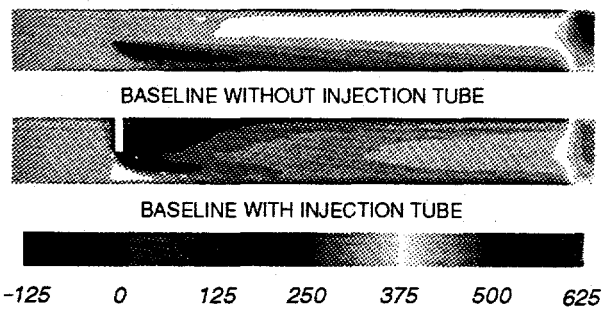

A. Axial Velocity (fps).

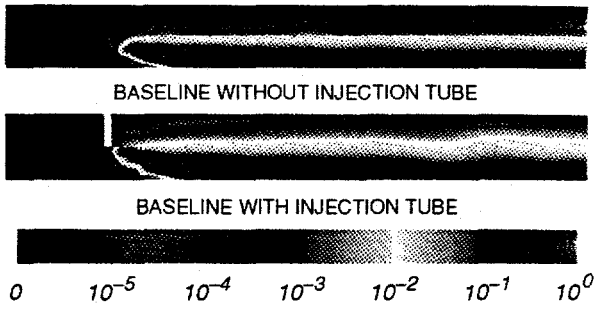

B. Fuel/Air Ratio.

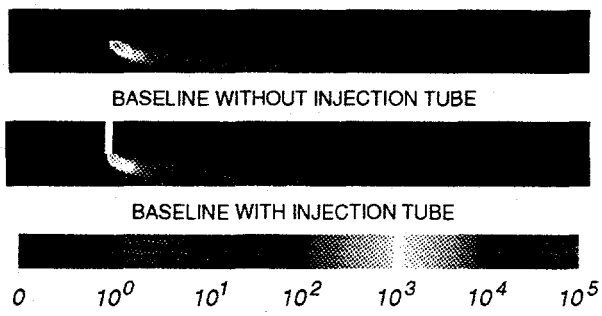

C. Fuel Droplet Population.

f/a_{min}	$f/a_{avg} \times 10^{-2}$	$f/a_{max} \times 10^{-1}$
BASELINE WITHOUT INJECTION TUBE		
2.1597×10^{-8}	2.6903	2.7039
BASELINE WITH INJECTION TUBE		
3.7385×10^{-5}	2.9617	2.4949

D. Exit Plane Fuel/Air Ratio.

Figure 3. Baseline Cases with and without Injection Tube.

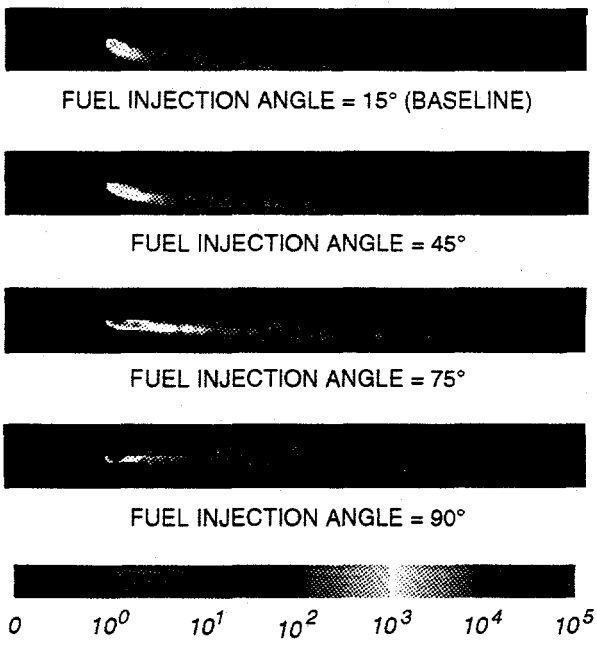

A. Fuel Droplet Population.

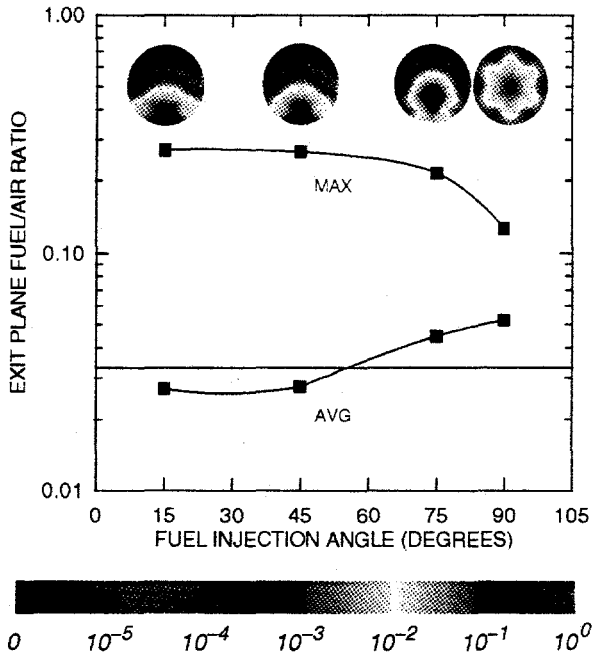

B. Exit Plane Fuel/Air Ratio.

Figure 4. Fuel Injection Angle Effects.

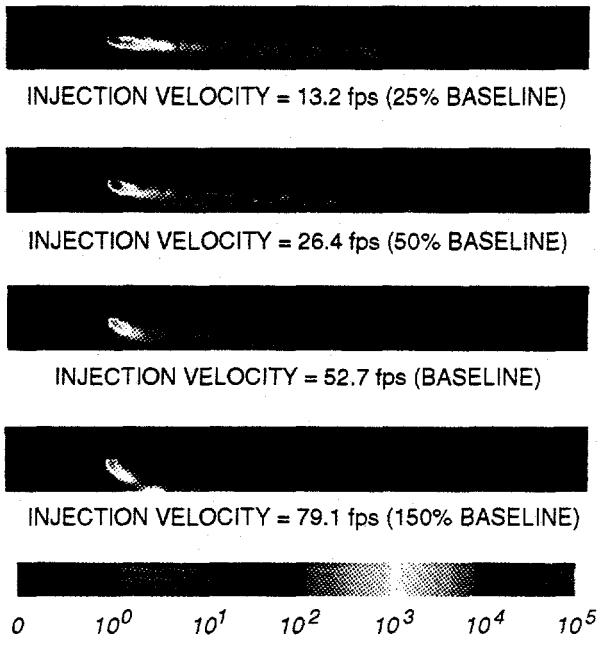

A. Fuel Droplet Population.

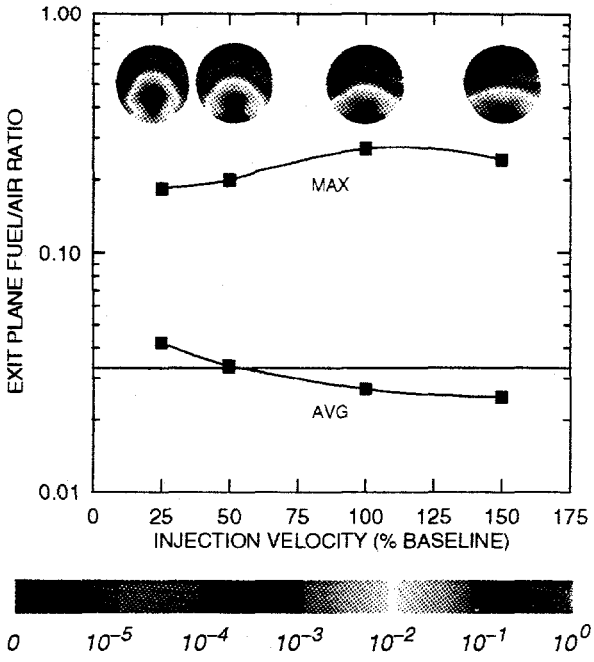

B. Exit Plane Fuel/Air Ratio.

Figure 5. Fuel Injection Velocity Effects.

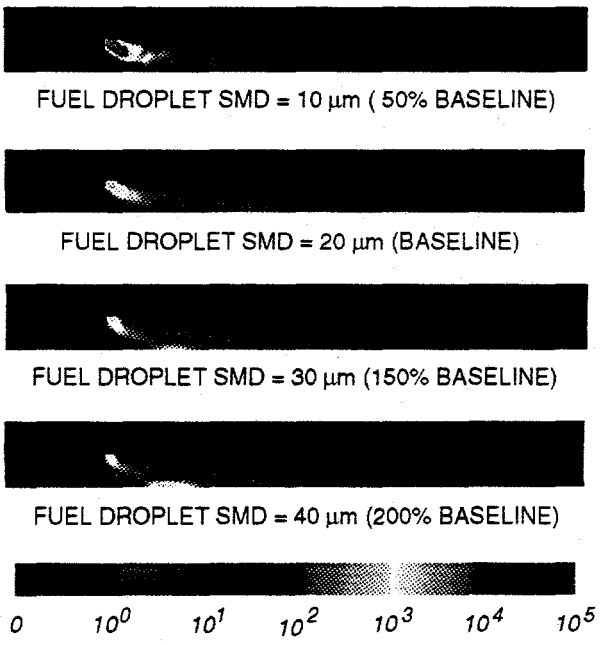

A. Fuel Droplet Population.

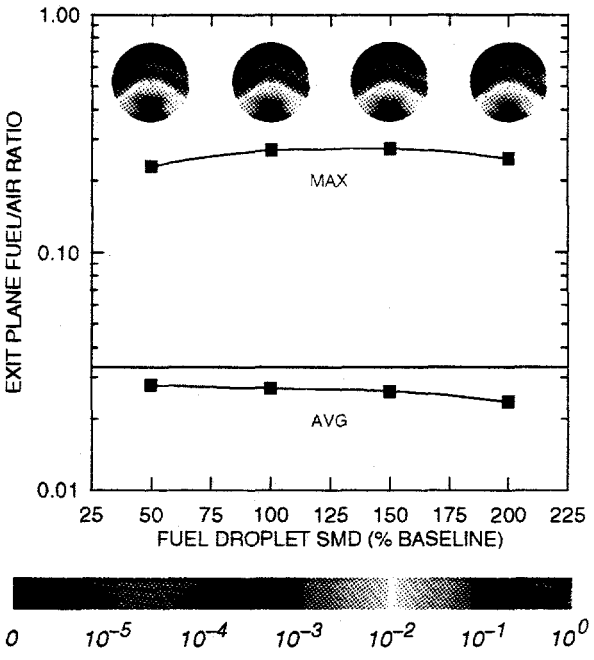

B. Exit Plane Fuel/Air Ratio.

Figure 6. Fuel Droplet SMD Effects.

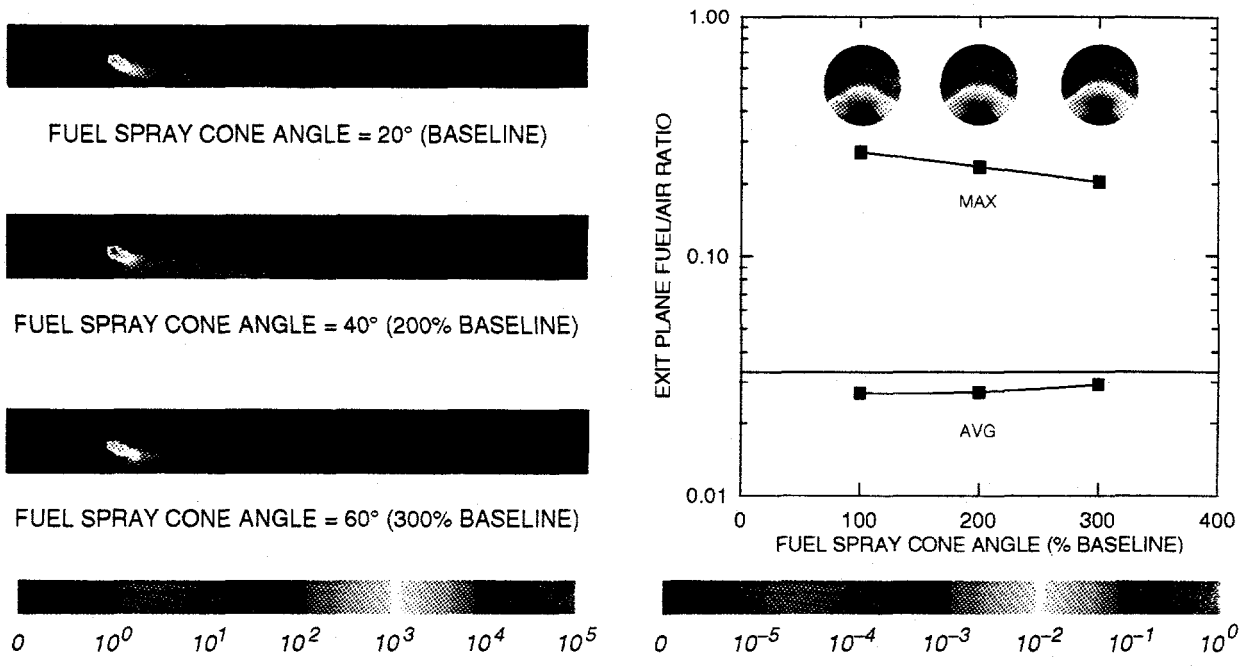

A. Fuel Droplet Population.

B. Exit Plane Fuel/Air Ratio.

Figure 7. Fuel Spray Cone Angle Effects.

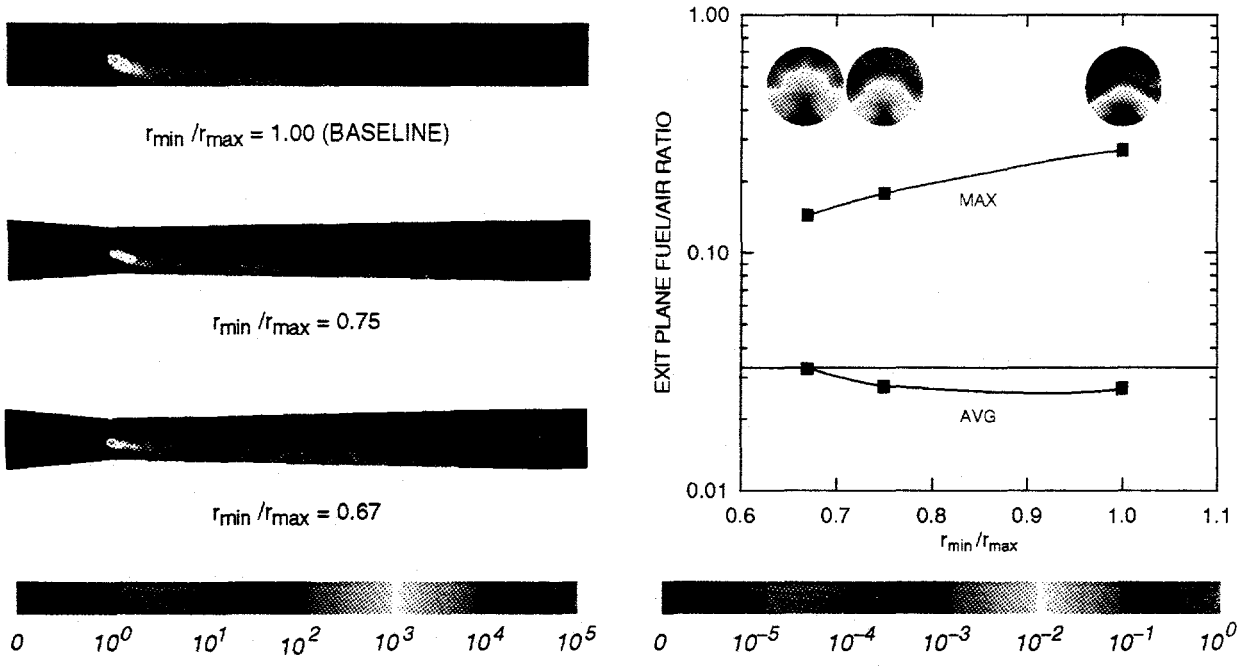

A. Fuel Droplet Population.

B. Exit Plane Fuel/Air Ratio.

Figure 8. Venturi Tube Effects.

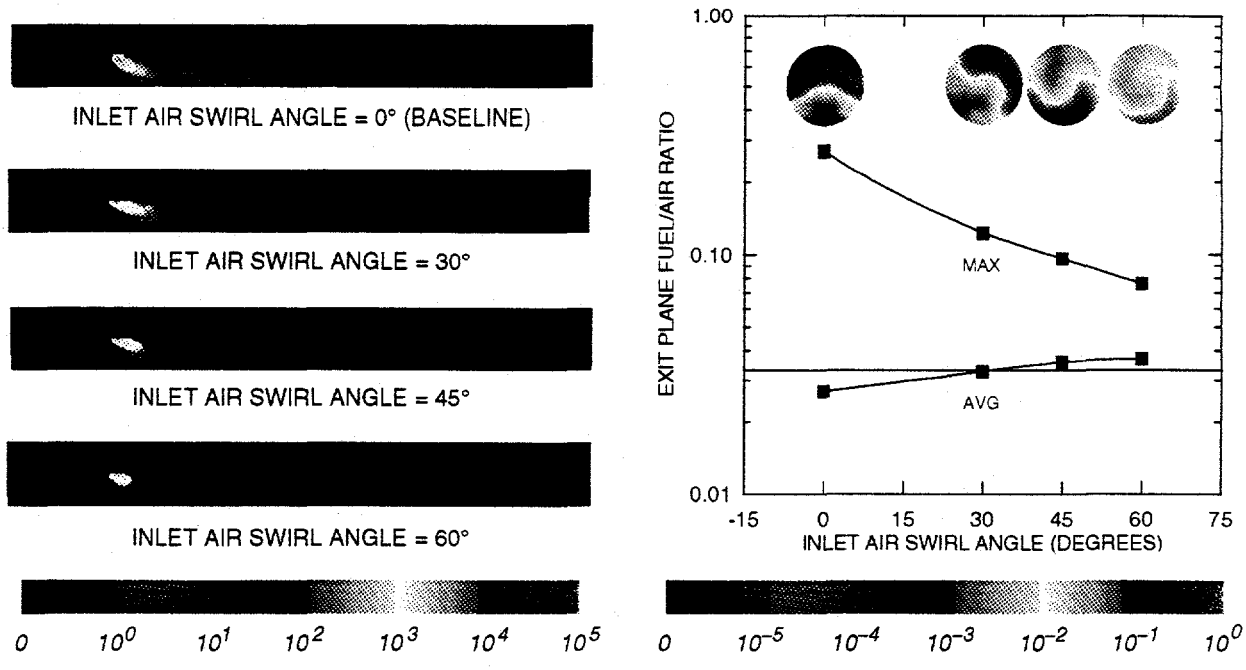

A. Fuel Droplet Population.

B. Exit Plane Fuel/Air Ratio.

Figure 9. Inlet Air Swirl Angle Effects.

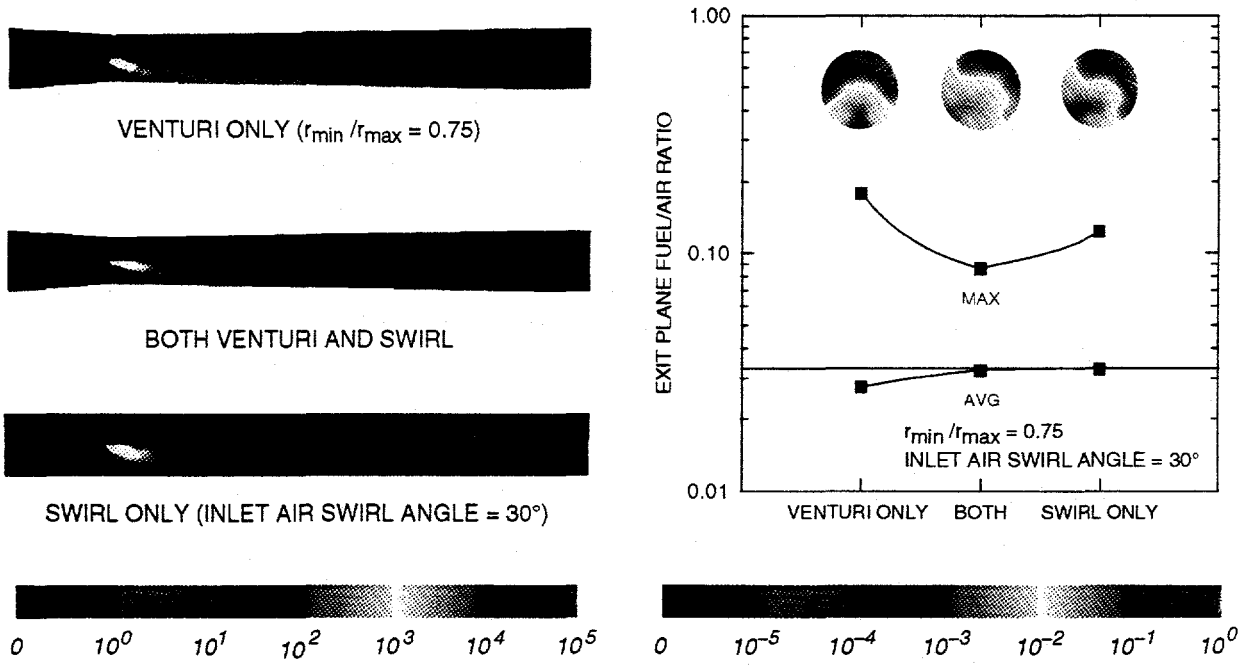

A. Fuel Droplet Population.

B. Exit Plane Fuel/Air Ratio.

Figure 10. Combined Venturi and Inlet Air Swirl Angle Effects.

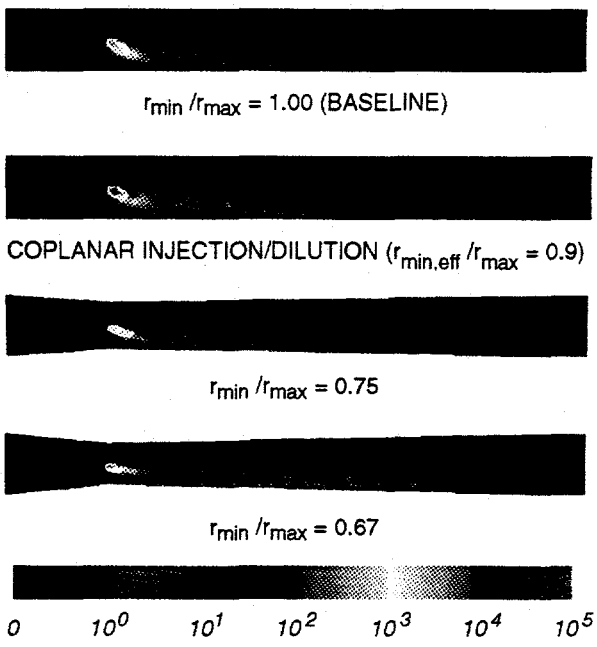

A. Fuel Droplet Population.

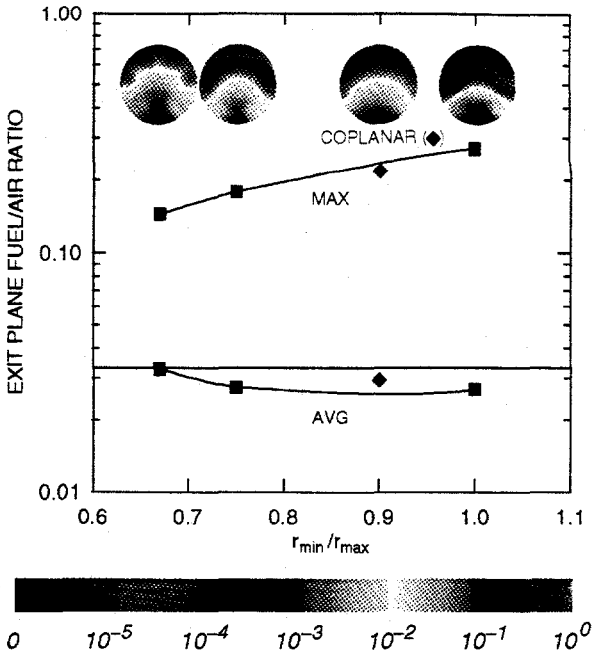

B. Exit Plane Fuel/Air Ratio.

Figure 11. Coplanar Injection/Dilution Effects.

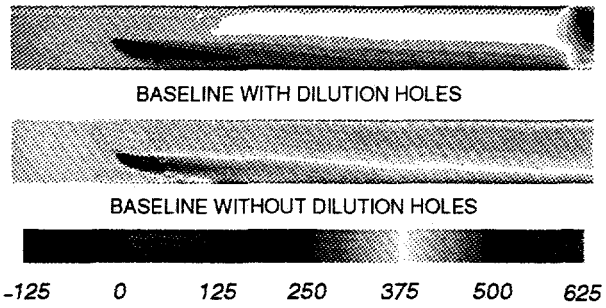

A. Axial Velocity (fps).

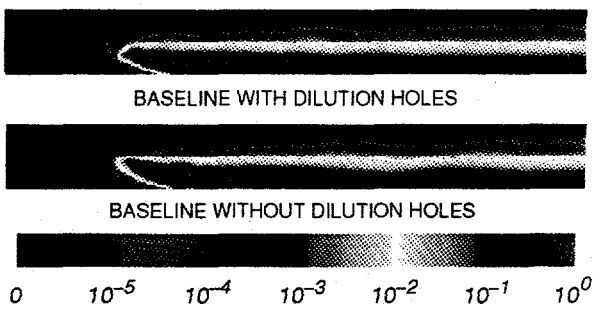

B. Fuel/Air Ratio.

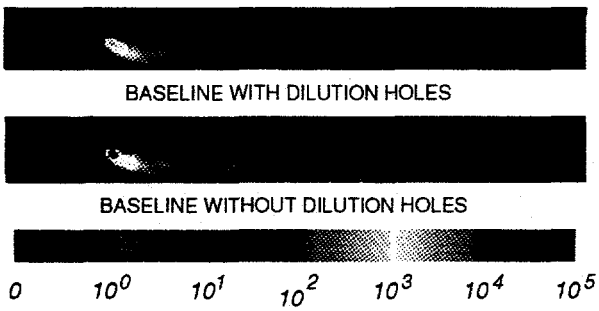

C. Fuel Droplet Population.

f/a_{min}	$f/a_{avg} \times 10^{-2}$	$f/a_{max} \times 10^{-1}$
BASELINE WITH DILUTION HOLES		
2.1597×10^{-8}	2.6903	2.7039
BASELINE WITHOUT DILUTION HOLES		
6.5459×10^{-9}	2.5602	2.8792

D. Exit Plane Fuel/Air Ratio.

Figure 12. Baseline Cases with and without Dilution Holes.

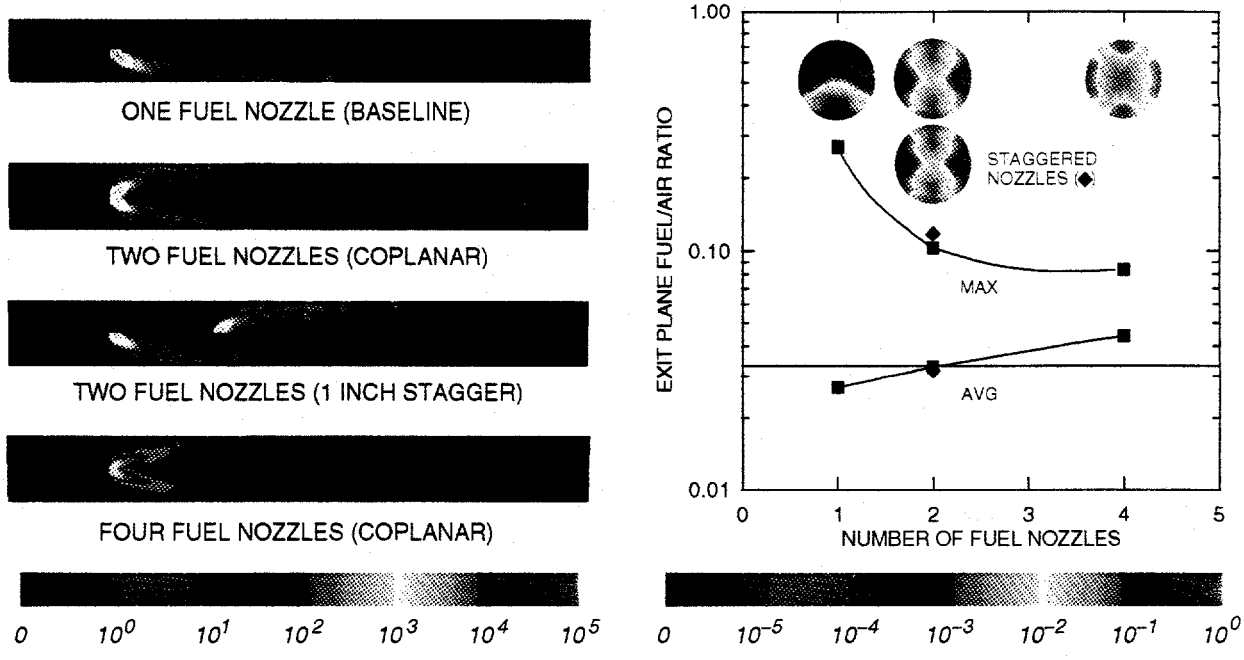

A. Fuel Droplet Population.

B. Exit Plane Fuel/Air Ratio.

Figure 13. Multiple Fuel Nozzle Effects.

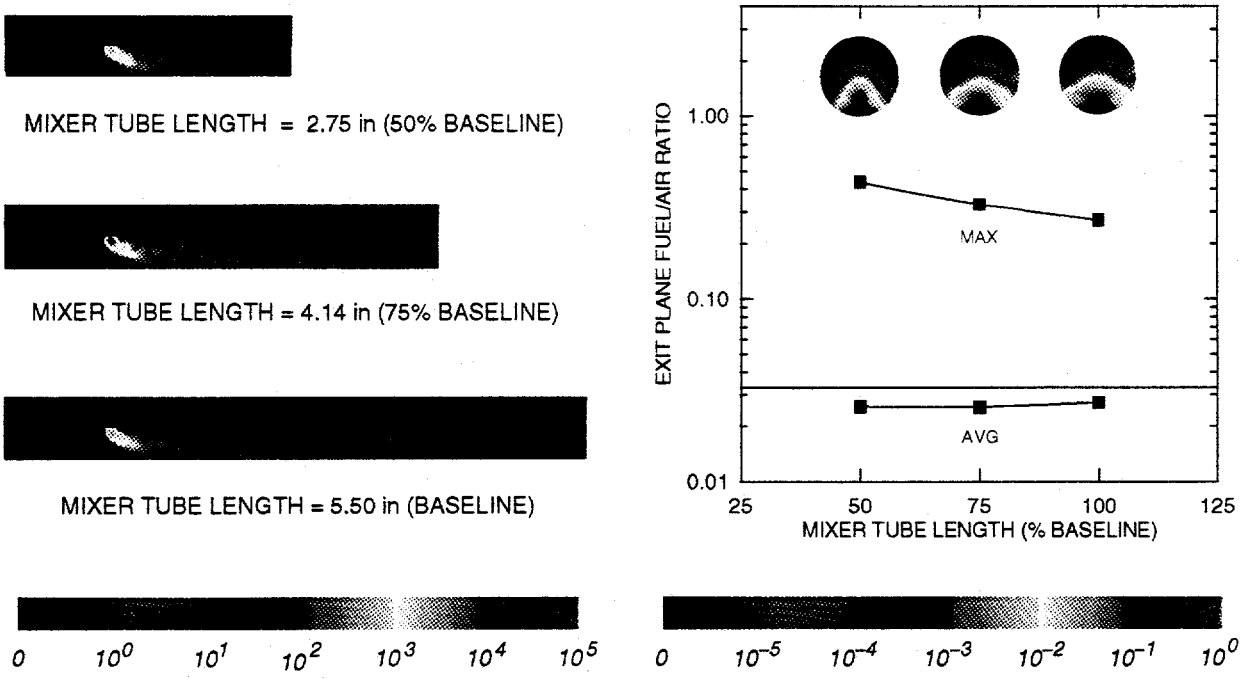

A. Fuel Droplet Population.

B. Exit Plane Fuel/Air Ratio.

Figure 14. Mixer Tube Length Effects.

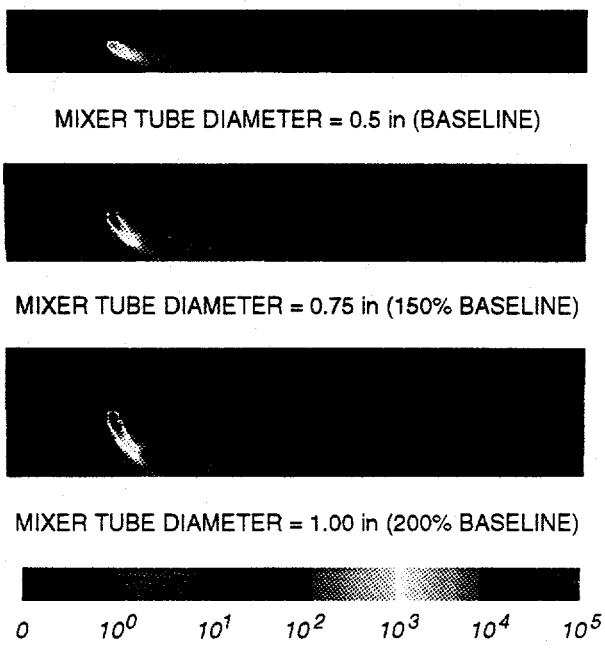

A. Fuel Droplet Population.

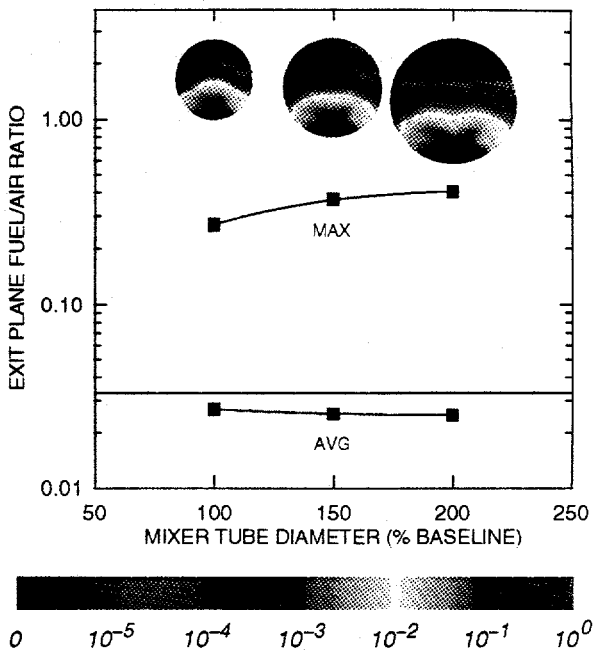

B. Exit Plane Fuel/Air Ratio.

Figure 15. Mixer Tube Diameter Effects ($\mathring{m}_{air}$ = constant).

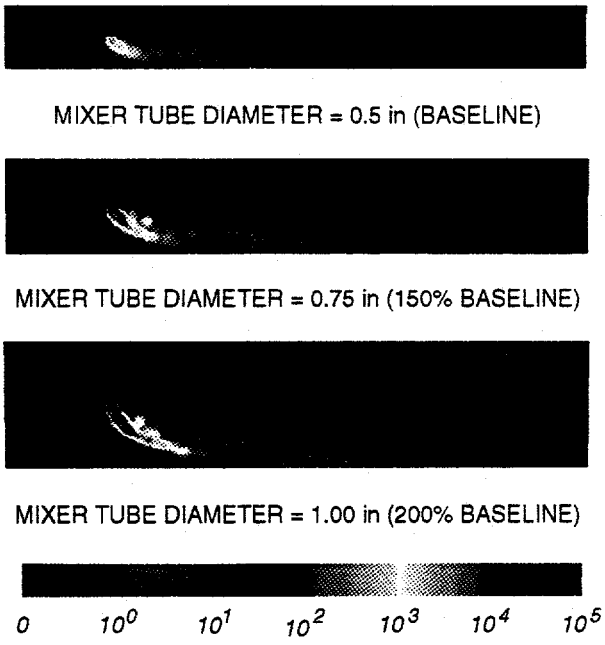

A. Fuel Droplet Population.

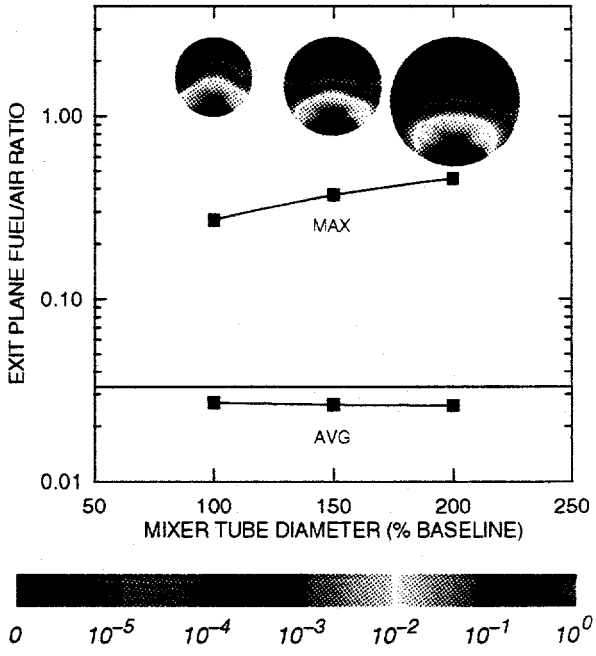

B. Exit Plane Fuel/Air Ratio.

Figure 16. Mixer Tube Diameter Effects (v_{air} = constant).

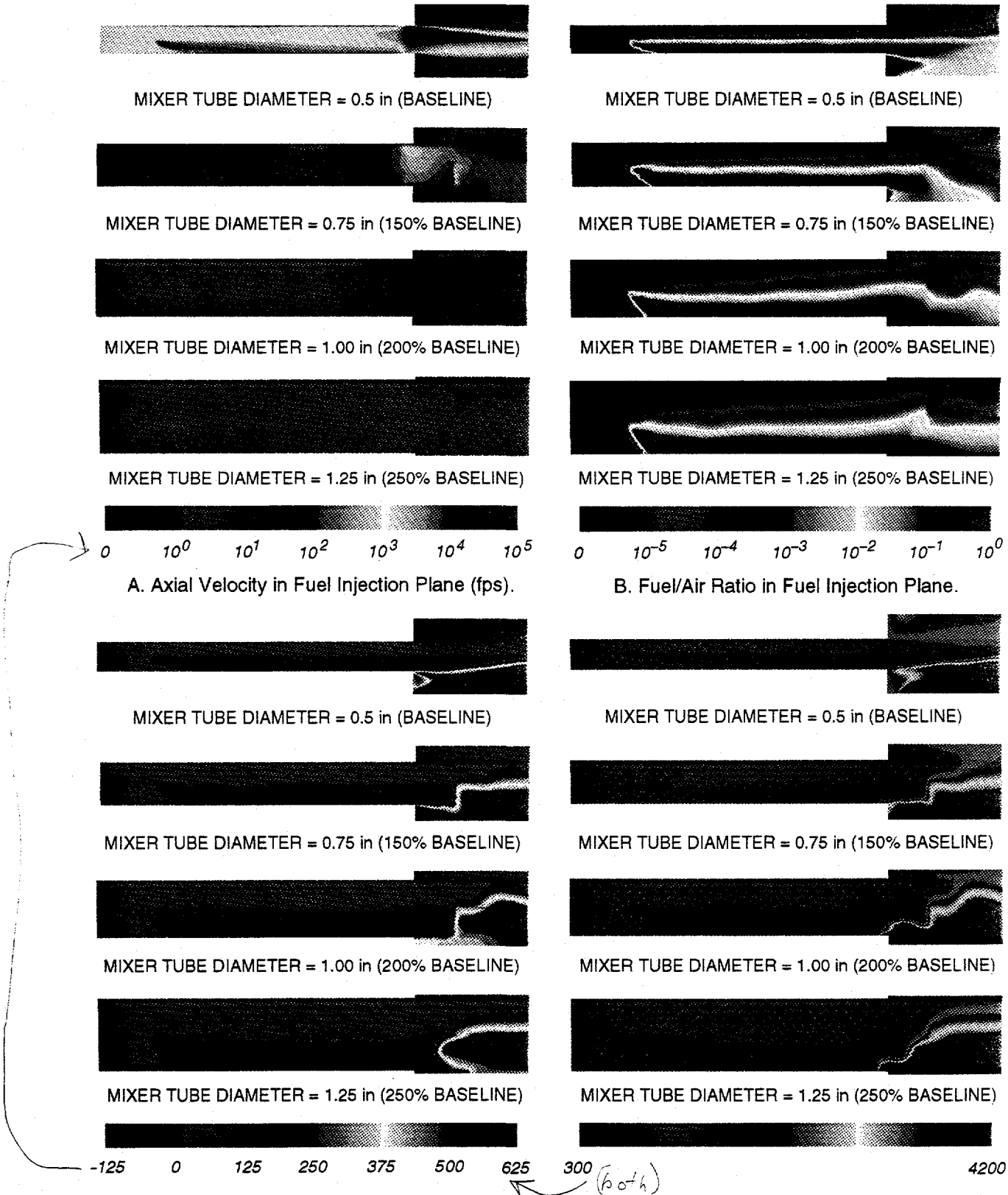

Figure 17. Mixer Tube Diameter Effects ($\dot{m}_{air}$ = constant): Combustion Results.

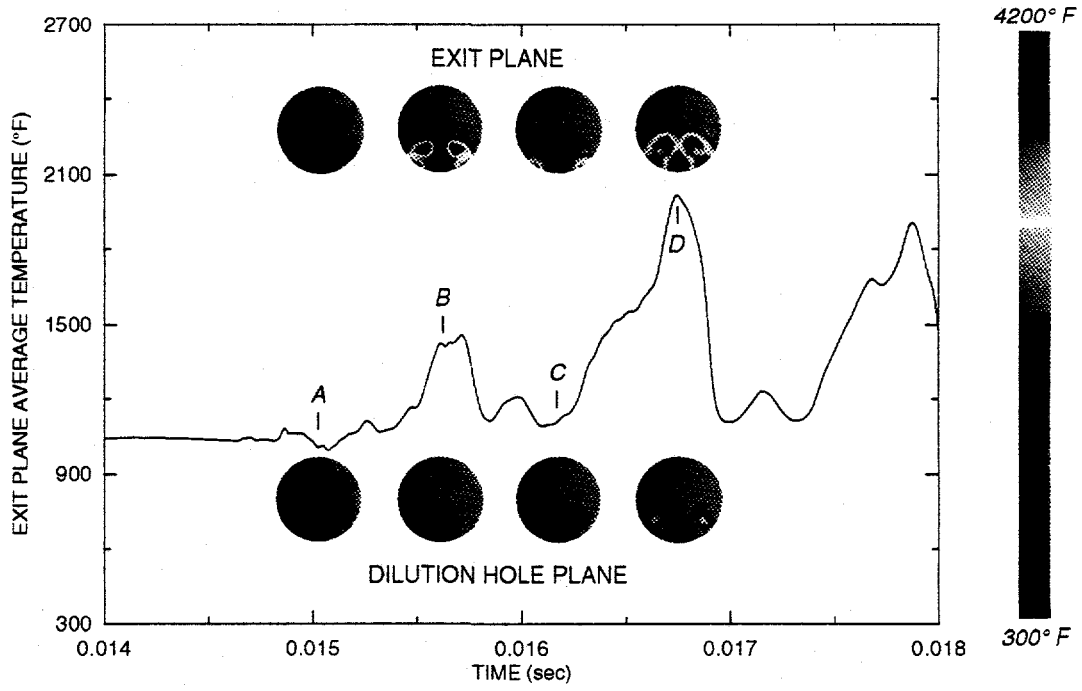

A. Time History.

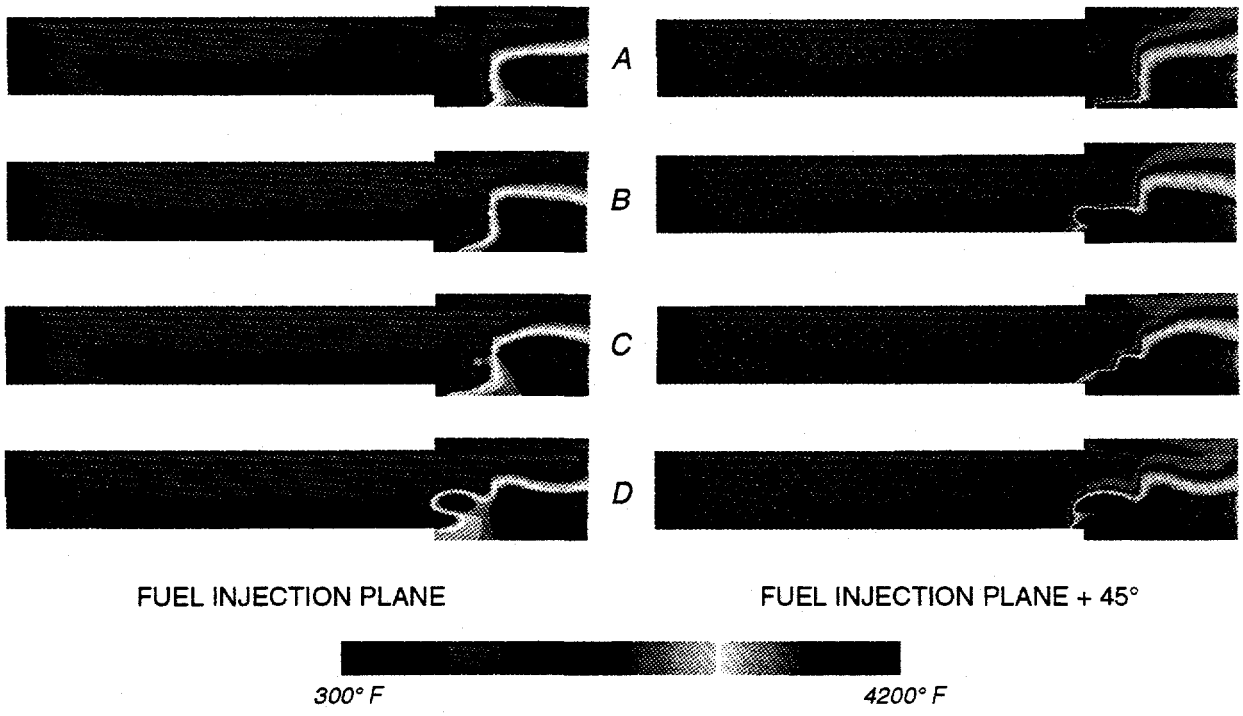

B. Temperature Profiles.

Figure 18. Flashback in 200% Baseline Radius Mixer Tube ($\dot{m}_{air}$ = constant).